Supplementary Material

1. SM-1: Details regarding the reflectance calculation for p-polarized light

The transfer matrix technique (TMM) is used for calculating the reflectance of p-polarized monochromatic light and is briefly presented here using Ref. [1–3]. All layers stacked along the z-axis are considered uniform, non-magnetic, and isotropic except the phosphorene layer [1,2]. The refractive index of the anisotropic phosphorene layer is calculated by the coordinate transformation method [2]. First, the rotation angle (φ) should be tuned by rotating the SPR sensor structure about the z-axis to match SPR excitation conditions [1–3]. The optimal rotational angle (φ) for each SPR structure is set at minimum reflectance value and maximum sensitivity. Once the φ is set—the range may lie in between 0 to 180 °—the incident angle θ is varied from 0-90° at each value of φ. After applying boundary conditions for tangential components of E and H fields, the characteristic matrix for the N-layer multilayer structure can be expressed as:

$$M = \prod_{k=2}^{N-1} M_k \tag{1}$$

where M_k denoted the matrix for kth layer and expressed as:

$$M_k = \begin{bmatrix} M_{11} & M_{12} \\ M_{21} & M_{22} \end{bmatrix} = \begin{bmatrix} \mathrm{Cos}\beta_k & \frac{-i\,\mathrm{Sin}\,\beta_k}{\rho_k} \\ -i\rho_k \mathrm{Sin}\,\beta_k & \mathrm{Cos}\,\beta_k \end{bmatrix} \tag{2}$$

Here, the term optical admittance β_k and phase factor ϱ_k of the kth layer is expressed as:

$$\beta_k = d_k \gamma_o (\varepsilon_k - n_1^2\,\mathrm{Sin}^2\theta_1)^{1/2} \tag{3}$$

and

$q_k = \sqrt{\frac{\mu_k}{\varepsilon_k}}\,Cos\theta$ for p-polarized light

where, θ_1 and γ_o indicates the incident angle and the free space wavenumber.

After following straightforward mathematical steps, the reflectance of N layered SPR sensor structure can be defined as [3]:

$$R_p = \left|\frac{(M_{11} + M_{12}\rho_N)\rho_1 - (M_{21} + M_{22}\rho_N)}{(M_{11} + M_{12}\rho_N)\rho_1 + (M_{21} + M_{22}\rho_N)}\right|^2 \tag{4}$$

Thus, reflectance curve may be plotted as R_p vs. incident angle using Equation (4). Further, different performance parameters described in Section 2 of the manuscript are analyzed through reflectance curves.

2. SM-2: Optimization of rotation angle (φ) for different Cu/Ni metal layer thickness combinations

A few Cu/Ni metal thickness combinations have been chosen to optimize the rotation angle (φ) for the proposed SPR sensor in terms of minimum reflectance, i.e., R_{min}, and maximum sensitivity, as shown in Figures S1-S11. The maximum sensitivity and R_{min} are achieved at the optimized value of φ, i.e., 72° with Cu and Ni thicknesses of 15nm and 80nm, respectively, as shown in Figure S9.

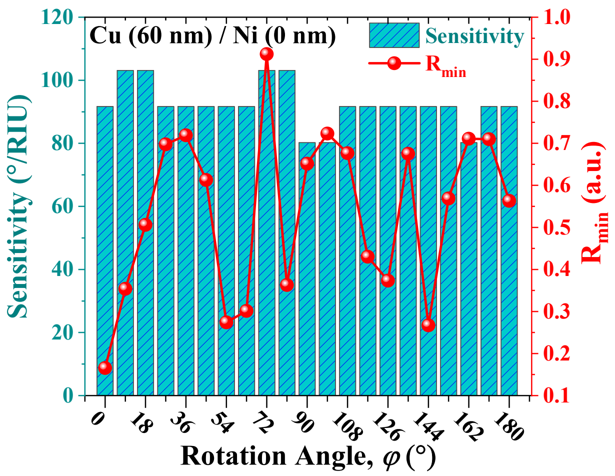

Figure S1. The sensitivity and R_{min} with different rotation angle at Cu (60 nm) / Ni (0 nm).

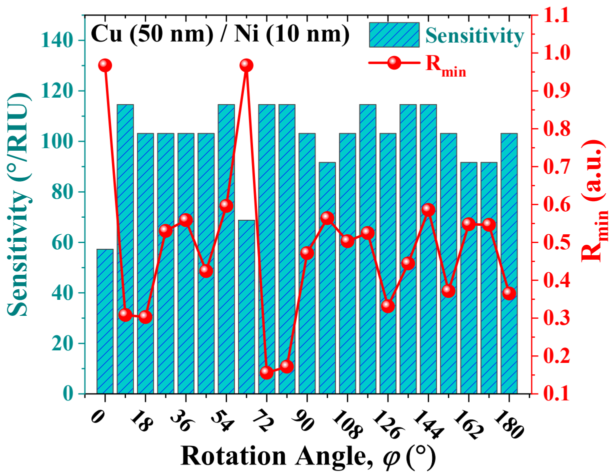

Figure S2. The sensitivity and R_{min} with different rotation angle at Cu (50 nm) / Ni (10 nm).

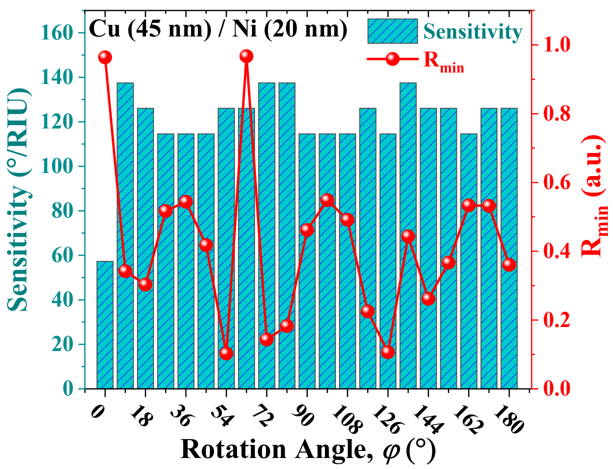

Figure S3. The sensitivity and R_{min} with different rotation angle at Cu (45 nm) / Ni (20 nm)

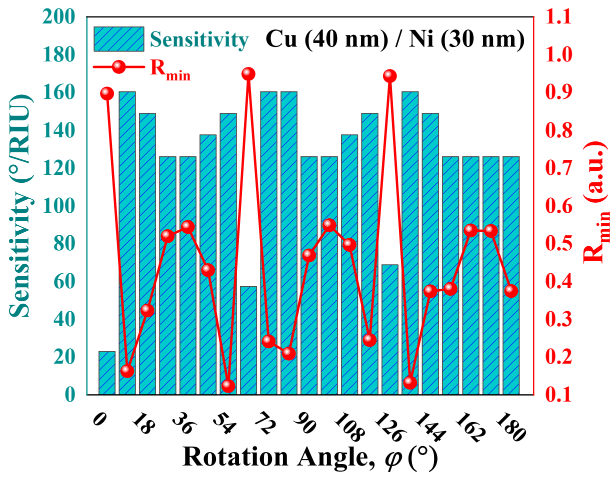

Figure S4. The sensitivity and R_{min} with different rotation angle at Cu (40 nm) / Ni (30 nm)

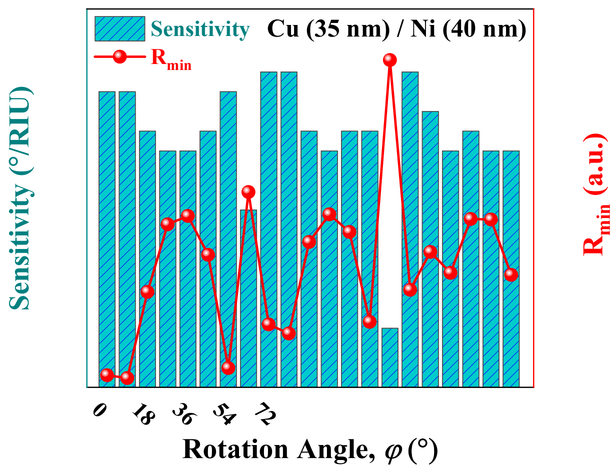

Figure S5. The sensitivity and R_{min} with different rotation angle at Cu (35 nm) / Ni (40 nm)

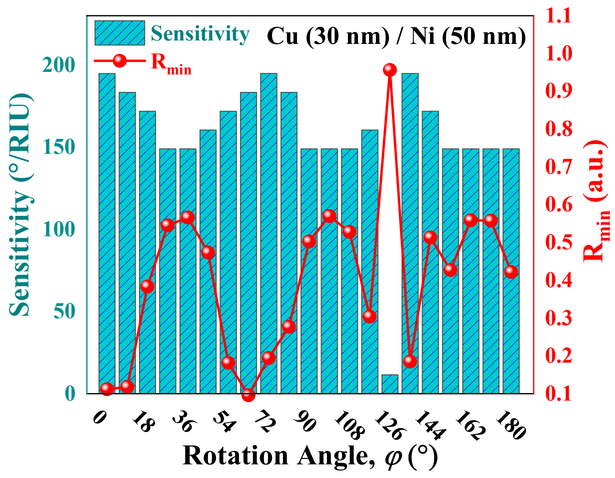

Figure S6. The sensitivity and R_{min} with different rotation angle at Cu (30 nm) / Ni (50 nm)

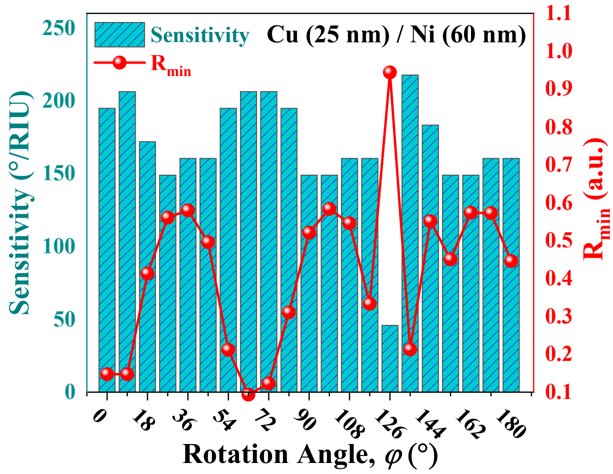

Figure S7. The sensitivity and R_{min} with different rotation angle at Cu (25 nm) / Ni (60 nm)

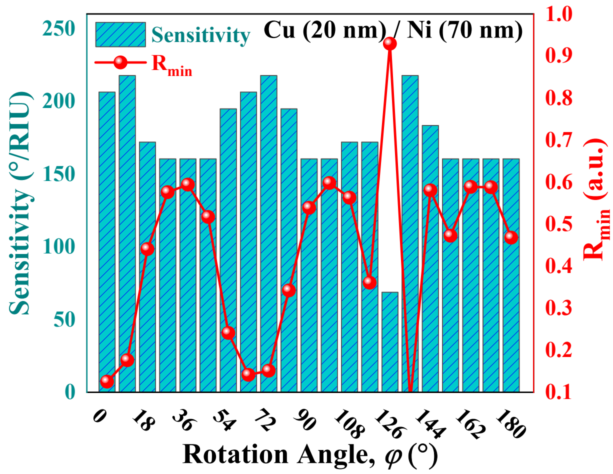

Figure S8. The sensitivity and R_{min} with different rotation angle at Cu (20 nm) / Ni (70 nm)

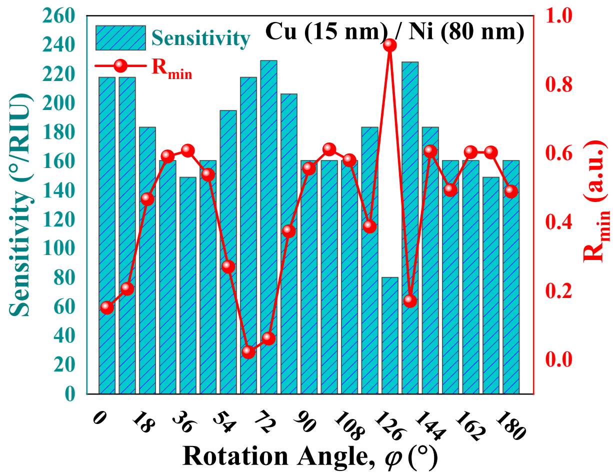

Figure S9. The sensitivity and R_{min} with different rotation angle at Cu (15 nm) / Ni (80 nm)

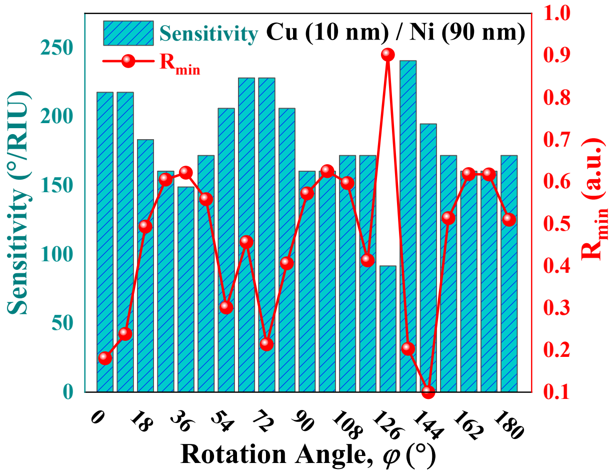

Figure S10. The sensitivity and R_{min} with different rotation angle at Cu (10 nm) / Ni (90 nm)

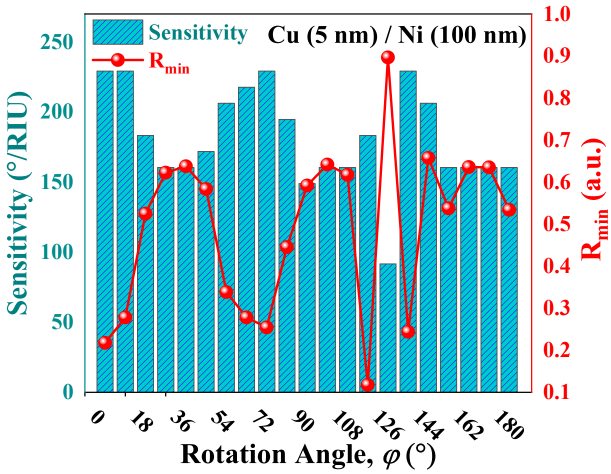

Figure S11. The sensitivity and R_{min} with different rotation angle at Cu (5 nm) / Ni (100 nm)

References

1. S. Pal, A. Verma, Y.K. Prajapati, and J.P. Saini, Sensitive detection using heterostructure of black phosphorus, transition metal di-chalcogenides and MXene in SPR sensor, *Appl. Phys. A.* **2020**, *126*, 809. https://doi.org/10.1007/s00339-020-03998-1.
2. Y. Yuan, X. Yu, Q. Ouyang, Y. Shao, J. Song, J. Qu, and K. T. Yong, Highly anisotropic black phosphorous-graphene hybrid architecture for ultrasensitive plasmonic biosensing: Theoretical insight, *2D Mater*. **2018**, *5*, 025015. https://doi.org/10.1088/2053-1583/aaae21.
3. M. K. Singh, S. Pal, A. Verma, V. Mishra, Y. K. Prajapati, Ultrasensitive Bi-metallic Surface Plasmon Resonance Biosensor Using Anisotropic Black Phosphorus and Antimonene nanomaterials, *Superlattices and Microstructures*, **2021**, *156*, 106969.